A Molecular Approach to Self-Assembly of Trimethylsilylacetylene Derivatives on Gold

Nathalie Katsonis,[a] Alexandr Marchenko,[a] Sébastien Taillemite,[a] Denis Fichou,*[a] Gaëlle Chouraqui,[b] Corinne Aubert,[b] and Max Malacria[b]

Abstract: We recently discovered that a linear multifunctional trimethylsilylacetylene (TMSA) compound forms long-range and highly stable self-assembled monolayers (SAMs) on reconstructed Au(111). To better understand the interactions governing self-assembly in this new system, we synthesized a series of homologue organosilanes and performed scanning tunneling microscopy (STM) measurements at the Au(111)/*n*-tetradecane interface. The four TMSA-terminated linear silanes that we synthesized self-assemble in similar ways on gold, with the molecules standing upright on the surface. In contrast, compounds with a slightly modified terminal group but the same polyunsaturated linear chain above the TMSA head do not self-assemble. In particular, substituting a methyl group of TMSA with a more bulky one prevents self-assembly. Removing the C≡C triple bond of TMSA or substituting the Si atom by a C atom also hinders self-assembly. Finally, substituting one methyl group of TMSA by a hydrogen atom induces self-assembly but in a different geometry, with the molecules lying flat on the gold surface in a quasi-epitaxy mode. Our molecular approach demonstrates the key role played by the TMSA head in self-assembly, its origin being twofold: 1) the TMSA layers are commensurate to the Au(111) adlattice along the ⟨112⟩ direction, and 2) the C≡C triple bond of TMSA activates the Si atom and induces the creation of a surface Si–Au chemical bond. The highly stable TMSA-based SAMs appear then as promising materials for applications in surface modification.

Keywords: chemisorption · nanostructures · organosilanes · scanning probe microscopy · self-assembly · silanes

Introduction

Self-assembled monolayers (SAMs) of organic molecules currently attract considerable attention, because of their potential applications in bio and chemical sensing, corrosion inhibition, wetting control, nanopatterning, and microelectronics.[1–8] They form a variety of 2D lattices, whose crystallographic structure depends on deposition conditions and substrate surface.[9–13] The most widely investigated self-assembled monolayer (SAM) compounds possess a sulfur-based anchoring group (mostly *n*-alkanethiols, dialkyl disulfides, or thioether) and are deposited on an atomically flat Au(111) surface. These organosulfur compounds chemisorb spontaneously on gold as organized monolayers through the formation of gold–sulfur bonds. A number of other SAMs based on non-sulfur molecules have been prepared and characterized, for example, alkylsilanes on SiO_2.[14, 15]

Beside chemisorption, through the formation of a covalent bond between a surface metal atom and an organic molecule (such as in the case of alkylthiols and gold), self-assembly usually results from weak molecule–substrate and molecule–molecule van der Waals interactions. A typical example of a physisorbed system is that of linear saturated *n*-alkanes that form various 2D self-assemblies at the *n*-tetradecane/Au(111) interface depending on their chain length.[16, 17] Self-assembly is then interpreted in terms of commensurability between the *n*-alkane lattice and the interatomic distance along the Au⟨110⟩ direction.

We recently reported[18] on the long-range SAM formation of 13-(trimethylsilyl)-1-tridecene-6,12-diyne (**1**) at the *n*-tetradecane/Au(111) interface. High-resolution scanning tunneling microscopy (STM) shows that this trimethylsilylacetylene (TMSA: -C≡C-Si$(CH_3)_3$) molecule spontaneously adsorbs on gold in an upright position, the trimethylsilyl group being in contact with gold. In contrast to reactive alkylsilanes such as R-SiH_3 recently reported by Owens et al.,[19] it is

[a] Dr. D. Fichou, N. Katsonis, Dr. A. Marchenko, S. Taillemite
CEA-Saclay, LRC Semi-Conducteurs Organiques
DSM/DRECAM/SPCSI
91191 Gif-sur-Yvette (France)
Fax: (+33) 1-69-08-84-46
E-mail: fichou@drecam.cea.fr

[b] G. Chouraqui, Dr. C. Aubert, Prof. M. Malacria
Laboratoire de Chimie Organique, UMR 7611
Université Pierre et Marie Curie
4 place Jussieu, 75252 Paris (France)

Supporting information for this article is available on the WWW under http://www.chemeurj.org or from the author: Experimental procedures for the synthesis of the molecules under study here.

DOI: 10.1002/chem.200204682

expected that SiR_4 compounds (such as **1**) do not chemically react with gold and do not form SAMs. However, compound **1** possesses a triple bond close to the trimethylsilyl group, as

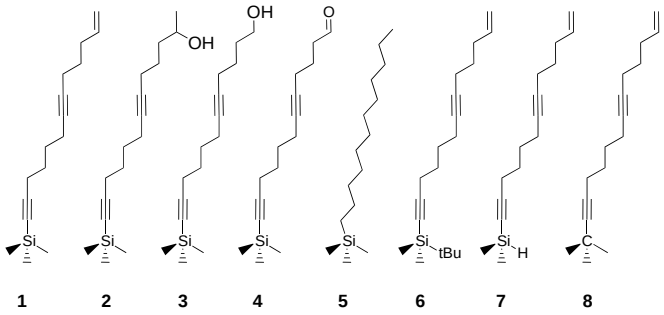

well as two other unsaturated bonds in its carbon chain that may influence self-assembly. Our preliminary results thus raise the essential question of the nature of the interaction between **1** and gold and suggest that a chemical reaction between Si and Au may have occurred. Such a chemical interaction would contribute to the long-range self-assembly, the stability, and the creation of pits, which we will describe below.

For the above-mentioned *n*-alkanes, in order to learn more about the nature of the interaction between silane **1** and Au(111), a series of homologous compounds with slightly modified chemical structures (**2**–**8**) was studied. Through such a molecular approach, we expect to be able to identify the key interactions that control adsorption and self-assembly of **1** on gold. As a first step to this approach, we have already reported that compound **8** (in which the silicon atom of **1** has been subsituted by a carbon) does not self-assemble on gold.[18] We attributed this result to the difference in size between the trimethylsilyl and *tert*-butyl end-groups, the latter being too small to allow commensurability of the organic and gold lattices. Furthermore, in contrast to silicon, carbon cannot adopt a pentacoordinat structure and, therefore, cannot be chemically linked to gold. In order to check these assumptions, we report here on the design and synthesis of a series of linear organosilanes derived from **1** and investigate by means of STM their ability to self-assemble at the Au(111)/tetradecane interface.

Silane **1** is a polyunsaturated molecule with a linear carbon chain (length ~19.5 Å) terminated by a trimethylsilyl group.[20] The triple bond close to the silicon atom rigidifies the -Si–C≡C–C- segment into a linear rod. We note that self-assembly of linear, conjugated arylthiols has recently been reported.[21] From a chemical point of view, the three multiple bonds of **1** can be considered as reactive sites that could be the basis of further chemical modification after deposition on a substrate. This is particularly the case for the terminal double bond (-CH=CH_2) which could be used to introduce a variety of functional substituants. In this respect, it has been recently shown that silane **1** is a very useful precursor for a variety of cobalt-mediated cycloaddition partners leading to functionalized polycyclic molecules.[22]

In compounds **2**–**4**, the terminal -C=CH_2 group of **1** has been transformed into -CH_2–CHOH–CH_3 (**2**), -CH_2OH (**3**), and -CH=O (**4**) functions, respectively, in order to check the influence of molecule–molecule interactions on self-assembly, while retaining the essential $(CH_3)_3$Si–C≡C- TMSA segment. Compound **5** essentially differs from **1** by the absence of the -C≡C- triple bond above the Si atom and will be useful to evaluate its importance on adsorption. In addition, compounds **6** and **7** have been selected to investigate how a slight modification of the size of the end-group (smaller with H in compound **7** and larger with *t*Bu in compound **6**) can affect the substrate–molecule interaction. Finally, molecule **8** allows a direct comparison between carbon and silicon as the central atom of the terminal group.

Results and Discussion

Synthesis of the silane derivatives: 1,3-Trimethylsilyl-tridec-1-ene-6,12-diyne (**1**) was prepared by following a procedure described elsewhere.[20] Silanes **2**–**4** were prepared from the reaction sequence depicted in Scheme 1. Sequential quantitative silylation of the triple bond of 2-(dodeca-5,11-diynyloxy)tetrahydropyran,[23] acid-catalyzed deprotection of the tetrahydropyranyl ether (quantitative), and Swern oxidation of the resulting alcohol **3** afforded the aldehyde **4** in 81% yield. Finally, addition of the methyl Grignard led to alcohol **2** in 78% yield.

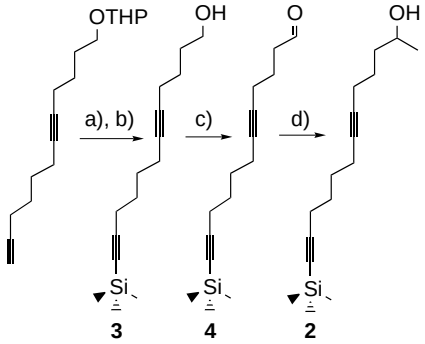

Scheme 1. Synthesis of trimethylsilyl-enediynes **2**–**4**. a) *n*BuLi, THF, −78 °C, $ClSiMe_3$, quant. b) cat. PTSA, MeOH, quant. c) $(COCl)_2$, DMSO, CH_2Cl_2, −78 °C to RT, 81%. d) MeMgBr, Et_2O, 0 °C, 78%.

Then, silylation of tridec-1-ene-6,12-diyne either with *tert*-butyldimethylsilylchloride or chlorodimethylsilane afforded the enediynes **6** and **7** in 84% and 69% yield respectively (Scheme 2).

Finally, compound **8** was prepared as outlined in Scheme 3. Alkylation of the lithium *tert*-butylacetylide with 2-(5-bromopentoxy)tetrahydropyran[24] provides the ether **9** in 74% yield. After deprotection, the resulting quite volatile alcohol **10** was oxidized[25] and then transformed into the dibromoolefin **11** in 43% yield over the two steps.[26] Reaction of **11** with *n*-butyllithium and consecutive alkylation with 2-(4-bromobutoxy)tetrahydropyran led to the corresponding ether in 31% yield. Subsequent acid hydrolysis yielded alcohol **12**,

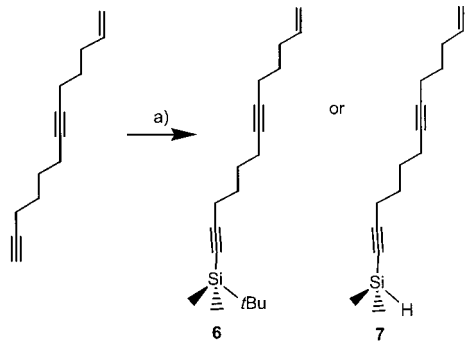

Scheme 2. Synthesis of enediynes **6** and **7**. a) *n*BuLi, THF, −78 °C; $ClSiMe_2tBu$, **6**: 84 % or $ClSiMe_2H$, **7**: 69 %.

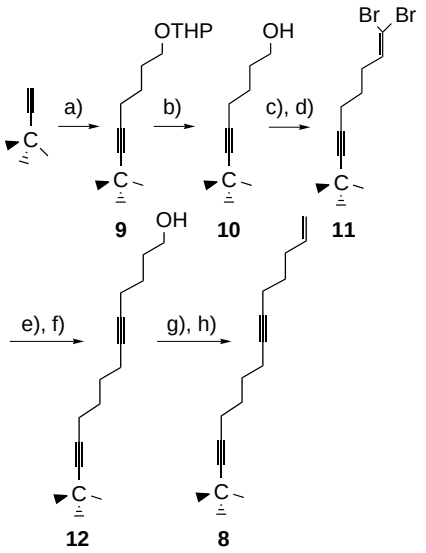

Scheme 3. Preparation of the *tert*-butylenediyne **8**. a) 1. *n*BuLi, −78 °C, THF; 2. HMPA, $Br(CH_2)_5OTHP$, 74 %. b) cat. PTSA, MeOH, 99 %. c) $(COCl)_2$, DMSO, CH_2Cl_2, −78 °C to RT. d) CBr_4, PPh_3, CH_2Cl_2, RT, 43 % overall. e) 1. *n*BuLi, −78 °C, THF; 2. HMPA, $Br(CH_2)_4OTHP$, 31 %. f) as b), 91 %. g) as c). h) *n*BuLi, Ph_3PCH_3Br, −78 °C to RT, 71 % overall.

which was then successively submitted to a Swern oxidation and a Wittig reaction to finally furnish **8** in 65 % overall yield.

Characterization of the Au(111)/*n*-tetradecane interface: The use of a liquid as tunnelling medium is particularly adapted to the STM study of molecules adsorbed on surfaces at ambient temperature. It allows both the deposition of the organic adsorbate and its local "in situ" observation.[27–29] Another advantage is that the high purity liquid in which the STM tip is immersed protects the tunnelling gap against humidity and pollution. Here we use high purity *n*-tetradecane, a nonpolar liquid with a low vapor pressure, which prevents rapid evaporation.

Reconstructed Au(111) is a major requirement to observe self-assembly. Unlike other fcc metal close-packed (111) surfaces, the Au(111) surface undergoes reconstruction when it is perfectly clean, such as when it is in ultra-high vacuum.[30] The ideality of the Au(111) surface can then be controlled by checking the presence of the $(23 \times \sqrt{3})$ superstructure. Importantly, this herringbone feature can be observed at the Au(111)/*n*-tetradecane interface as shown in Figure 1. For

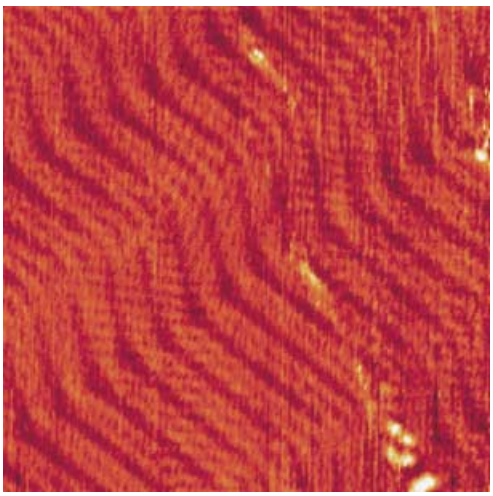

Figure 1. Typical STM image (80×80 nm^2; $I_t = 90$ pA; $U_t = 215$ mV) of a reconstructed Au(111) surface recorded in *n*-tetradecane at ~293 K. The herringbone feature throughout the image corresponds to the reconstruction stripes of gold. At this temperature, individual *n*-tetradecane molecules are also visible and are adsorbed in lamellae along the gold stripes.

temperatures below 293 K, it is even possible to observe the individual *n*-tetradecane molecules lying flat on Au(111), the thickness of the adsorbed *n*-tetradecane monolayer being about 1.5 Å. Adsorbed *n*-tetradecane molecules align along the reconstruction stripes of gold and adopt a lamellar structure. When organic molecules are solvated in *n*-tetradecane, preferential adsorption of these molecules takes place if they have a higher molecular weight than *n*-tetradecane and/or a higher affinity with reconstructed Au(111).[16, 31] For temperatures higher than 293 K by 2–3 degrees, STM shows that *n*-tetradecane does not adsorb on gold anymore (although the bare surface still exhibits the typical reconstruction stripes).

Self-assembly of TMSA-terminated molecules 1–4: As for silane **1**, deposition of a monolayer of the other three TMSA-terminated compounds **2**, **3**, and **4** on reconstructed Au(111) results in the same network of randomly distributed pits (Figure 2). The STM images show that these organized monolayers extend over several hundreds of nanometers. The pit-like structure is not observed with compounds **5**–**8**, which either do not self-assemble or self-assemble in a different fashion (see below). As we expected, these results confirm the importance of the TMSA termination in the adsorption and self-assembly of compounds **1**–**4**.

The depressions created in the monolayers of molecules **1**–**4** have a constant depth of 2.4 Å equal to a single atomic Au(111) step height (Figure 2b). Very similar pit holes are observed for *n*-alkanethiol monolayers adsorbed on Au(111),[32] which, notably, also have the same depth of 2.4 Å.[33] These depressions are usually interpreted as vacancies in the gold layer rather than defects in the *n*-alkanethiol layer.[34] The commonly accepted interpretation for their formation in the case of alkanethiols is that the chemical bond between the sulfur and the gold atoms leads to the etching of some atoms from the Au(111) surface.[10] By analogy, the

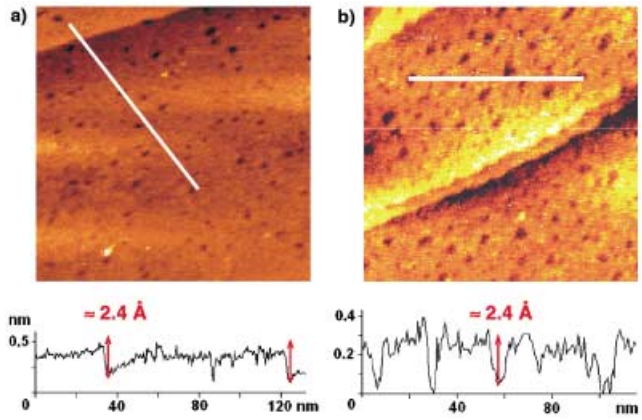

Figure 2. Typical STM images of two monolayers of TMSA compounds at the reconstructed Au(111)/*n*-tetradecane interface. a) Compound **2** (175×175 nm^2; $I_t = 90$ pA; $U_t = 210$ mV). b) Compound **4** (170×170 nm^2; $I_t = 96$ pA; $U_t = 500$ mV).

presence of etch-pits in SAMs of TMSA compounds strongly suggests the existence of a chemical bond between the molecules and the Au(111) surface.

In contrast to *n*-alkanethiols, which form numerous metastable structures on Au(111), SAMs of compounds **1**–**4** are free of grain boundaries (within the limits of individual gold terraces) and are homogeneous over distances of several hundreds of nanometers. In order to reach a minimum interaction energy, *n*-alkanethiol molecules occupy the same adsorption sites on Au(111), but adopt slightly different molecular planes in the unit cell. This structural restriction creates strains and domains, thus inhibiting the formation of a long-range two-dimensional order. Therefore, the absence of grain boundaries for TMSA compounds **1**–**4** suggests that the organic overlayers are commensurate to the Au(111) lattice.

Moreover, molecule–molecule interactions probably also play a role in the self-assembly of TMSA-silane/Au(111) systems. Organic molecules deposited on Au(111) can interconnect by lateral interchain mechanisms, such as π stacking, hydrogen bonding, dipole coupling, or covalent attachment.[35] Multiple unsaturated bonds and oxygen-containing groups in silanes **1**–**7** along the chain or at the distal end suggest contributions of π stacking interactions and hydrogen bonding. In addition, it is worth noting that the double and triple bonds, if not conjugated, also rigidify the chains and thus further stabilize the self-assembly.

Structure of the TMSA monolayers on gold: High-resolution STM images of TMSA compound **1** show a close-packed hexagonal arrangement (Figure 3a). The lateral repeat distance between molecules is quantified in the cross-sectional profile and equal to 5.0 ± 0.1 Å. Since this distance corresponds to the diameter of the TMS group,[36] it suggests that each molecule has an overall linear conformation and stands nearly upright on the surface. Another argument in favor of such a vertical position is the circular shape of the molecular spots on the STM images, which are incompatible with molecules lying flat on gold. The distance between neighboring molecules (~5 Å) is close to $T\sqrt{3}$, whereby $T = 2.88$ Å is the interatomic distance on the Au(111) surface. The separation between neighboring molecules appears then to be precisely the distance between second-neighboring ⟨110⟩ Au rows. This means that molecules of **1** are bound either in

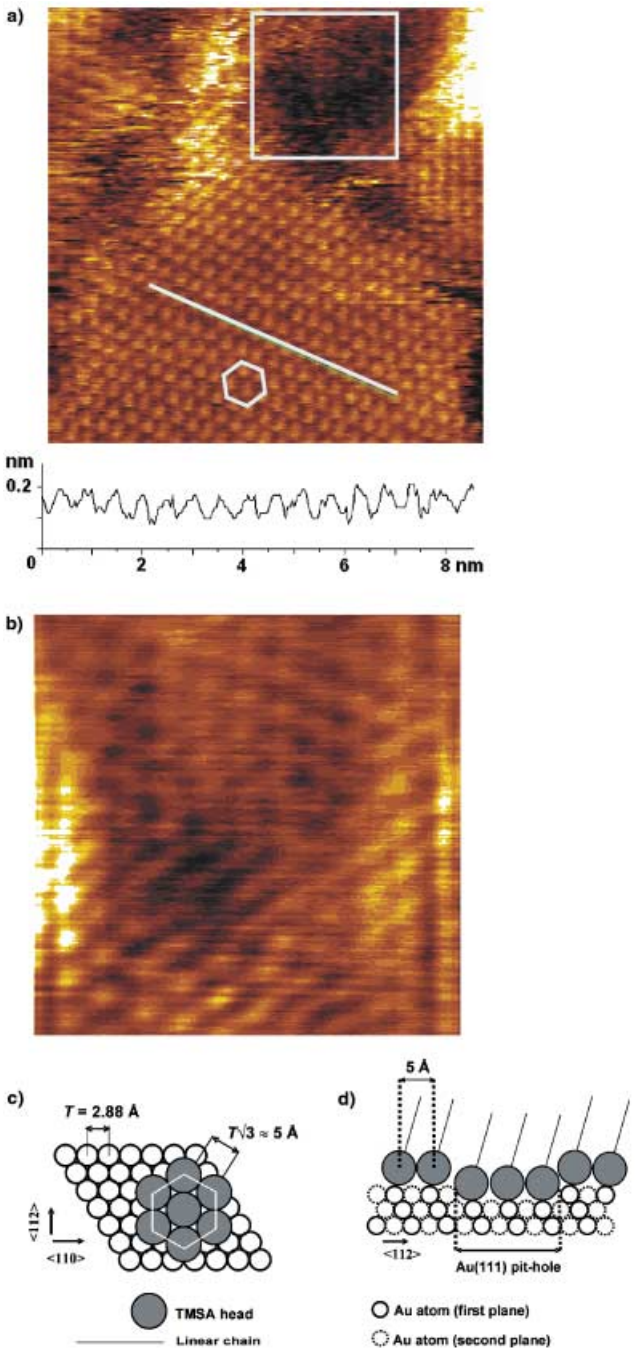

Figure 3. a) High-resolution STM image (14×14 nm^2; $I_t = 150$ pA; $U_t = 250$ mV) of a self-assembled monolayer of TMSA **1** at the Au(111)/*n*-tetradecane interface. The unit cell is indicated by a white hexagon. The cross-sectional profile below the image was recorded along the white line. The dark area inside the white square in the upper right part of the image corresponds to a pit hole whose inner structure is shown in b. b) Magnification of the square area (5.5×5.5 nm^2) filtered through a Fourier transform treatment. c) Top view of one of the two possible hexagonal arrangements of the commensurate $\sqrt{3} \times \sqrt{3}(R30^\circ)$ overlayer of **1** on Au(111). Here, the molecules occupy the top-sites of gold atoms. d) Side-view along the ⟨112⟩ gold axis of the overlayer of **1** on Au(111) showing a pit hole. Gold atoms are located alternately in the front (full circles) and back (dashed circles) planes parallel to this page.

equivalent threefold hollow sites or on top sites of Au(111), for which the same lattice vectors are expected. In both cases, adlattice of **1** is then perfectly commensurate with the Au(111) lattice along the ⟨112⟩ direction as representated on Figure 3c. Monolayers of **1** adsorbed on Au(111) form a so-called $(\sqrt{3} \times \sqrt{3})R30^\circ$ structure with lattice vectors ($a = b = 5 \pm 0.2$ Å).

The STM image in Figure 3b results from a Fourier transform filtering of the etch-pit area inside the white square of Figure 3a. It reveals the presence of a hexagonal structure inside the pit that has the same lattice vectors than the molecular adlattice. It demonstrates that the pit holes are also covered with self-assembled molecules. This is in agreement with the assumption that these depressions do not correspond to molecular vacancies in the organic monolayer, but rather to vacancies in the Au(111) layer (Figure 3d).

Under our experimental conditions, monolayers of **1** are stable for several hours without observed changes. After four hours, the solvent had evaporated, leaving a dry film with the same hexagonal molecular packing on the gold surface (Figure 4a). The stability of the layer should thus be a consequence of a static anchoring of the molecules.

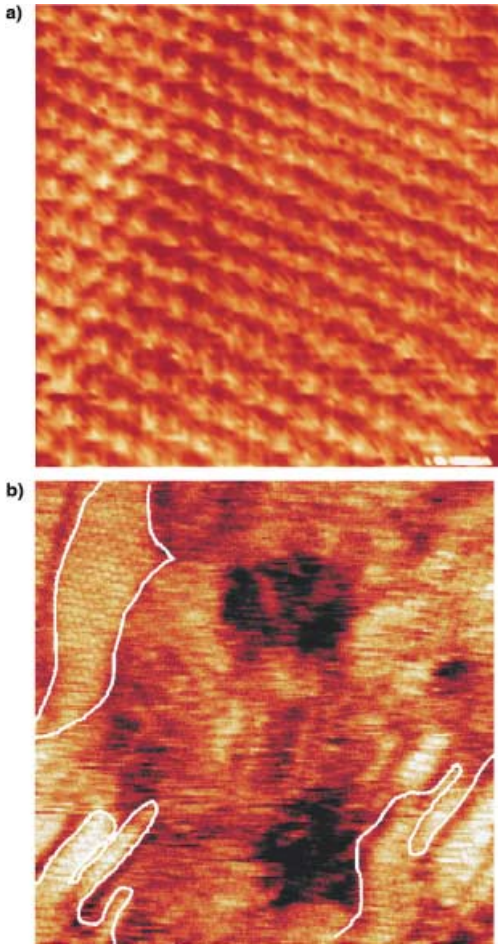

Figure 4. a) STM image (6.7×6.7 nm^2; $I_t = 150$ pA; $U_t = 250$ mV) of a dry film of **1** on Au(111) recorded after complete evaporation of *n*-tetradecane. b) STM image (30×30 nm^2; $I_t = 33$ pA; $U_t = 1.612$ V) of a monolayer on Au(111), obtained by deposition of a mixture (50:50 *v*/*v*) of silane **1** and *n*-dodecanethiol in *n*-tetradecane. The white lines delineate the domains inside which silane **1** self-assembles.

To evaluate the stability of silane **1**, we performed co-adsorption experiments with *n*-dodecanethiol on Au(111). Figure 4b is a large-scale STM image of a mixed monolayer obtained after deposition of a 50:50 (v/v) mixture in *n*-tetradecane with a concentration of about 0.05 mg mL^{-1}. The three inner domains, delineated by the white lines, exhibit the same hexagonal structure as in Figure 3a and can be attributed to silane **1**. The rest of the scanned area is rather disordered, with the exception of some local preferential alignments that can be attributed to *n*-dodecanethiol. As a matter of fact, it has already been reported that *n*-dodecanethiol monolayers on Au(111) usually form small domains organized in a $c(4 \times 2)$ superstructure.[9, 10] Given that the respective 2D-lattices of silane **1** and *n*-dodecanethiol do not fit together, this image highlights the exceptional self-assembling properties of silane **1** on gold; this can be compared with SAMs that are commonly used in numerous applications.[37] However, our STM images do not allow us to evaluate precisely the respective proportions of silane **1** and *n*-dodecanethiol in the mixed monolayer composition, although it seems to be similar to the 50:50 (v/v) ratio of the starting solution in *n*-tetradecane.

Self-assembly of silanes 2–4: Figure 5a shows a small-scale image of TMSA compound **2** on Au(111). It is also typical of images obtained with compounds **3** and **4**, all three bearing a distal end-group that contains an oxygen atom (alcohol or aldehyde) instead of the vinyl group of **1**. In spite of repeated attempts, STM resolution at the molecular level was never as clear as that obtained with compound **1**. This can be attributed to the structure of the molecule itself, whose higher polarizability enhances the interaction with the intense and non-homogeneous electric field in the STM tunelling gap. However, analysis of Figure 5a shows that the monolayer is made of parallel rows separated by a distance of ~ 10 Å, a distance approximately double of that between molecules **1** (see Figure 3a). This suggests that individual molecules of **2** are paired through hydrogen bonds between their respective OH groups, as has been reported recently by Xu et al. for chlorophile derivatives.[38] This pairing would then lead to the apparent substructure of parallel alignments masking the underlying hexagonal packing.

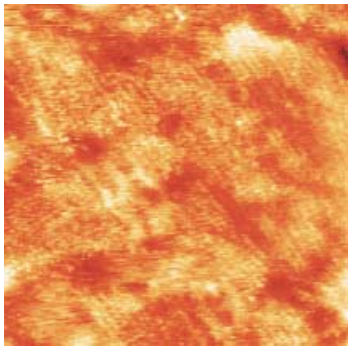

Figure 5. a) STM image (60×60 nm^2; $I_t = 100$ pA; $U_t = 0.323$ V) of silane **2** at the Au(111)/*n*-tetradecane interface. Higher STM resolution is intrinsically hindered due to the high polarizability of the distal OH group of silane **2**.

Non-TMSA compounds 5–8 on Au(111): In molecules **5**–**8**, the TMSA head group has been slightly modified so that the influence of each of its subunits on self-assembly can be studied independently. The triple bond is suppressed in **5**, one methyl group is changed into a *tert*-butyl group in **6** and into an hydrogen atom in **7**, and finally the silicon atom is changed into a carbon one in **8**. Except for silane **5**, we have been able to keep the same polyunsaturated chain as that of silane **1**.

Under our experimental conditions, the STM images at the *n*-tetradecane/Au(111) interface never show any evidence of self-assembly for molecules **5**, **6**, and **8**. In contrast, silane **7** self-assembles on gold, but adopts a different geometry as compared to silane **1** (see below). The absence of self-assembly for molecule **8** confirms the key role played by the Si atom through 1) the size of the TMS group (commensurability) and 2) its chemical reactivity with gold (pentacoordinated complex). In addition, the disordered films obtained with **5** confirms that the π-electrons rich C≡C triple bond is necessary to activate the reactivity of Si towards Au. Finally, the absence of self-ordering for molecule **6** can be attributed to the steric hindrance introduced by the bulky *tert*-butyl group, which prevents the Si atom from being sufficiently close to the gold surface.

The case of silane **7** is particularly demonstrative. Replacement of one methyl by a hydrogen atom is expected to induce chemisorption on Au(111) for two reasons. First it allows the Si atom to get closer to the gold surface and second it makes Si more reactive towards gold. Figure 6a reveals a mosaiclike structure that contains separated domains with highly ordered stripes (or lamellae) aligned along three preferential directions oriented at 120°. Given that the Au(111) surface has a threefold symmetry and thus possesses three physically equivalent directions, one can assume that the monolayer of **7** is in quasi-epitaxy with Au(111). Figure 6b is a small-scale image of the SAM. The overlayer consists of a close-packed arrangement of lamellae separated by troughs; it also contains some packing defaults that sometimes break or bend the lamella. STM images show that in most of the monolayer area the width of these lamellae is ~2 nm, as shown by the cross-sectional profile. This lamella width corresponds to the length of molecule **7**, indicating that molecules lie flat on the surface, with their main axis perpendicular to the lamellae direction. However, in some restricted regions (e.g., in the upper-right part of Figure 6b) lamellae shorter than 2 nm are also observed. We know that in the case of nonsymmetric linear molecules (such as compound **7**), head-to-head or head-to-tail arrangements can coexist. It appears that self-assembly of **7** essentially generates a head-to-tail arrangement with a minor contribution of a head-to-head one (see scheme in Figure 6c).

Remarkably, the reconstruction stripes of Au(111) are not visible on any of the images of molecule **7** that we recorded. This is in contrast with adsorption of long-chain aliphatic compounds physisorbed on Au(111). It has been recently reported[5, 16, 17] that long-chain *n*-alkanes physisorbed on Au(111) are "transparent" to reconstruction lines. The lifting of Au(111) reconstruction through a monolayer of molecule **7** (and also of TMSA compounds **1**–**4**) is typical of chemisorption and can be considered as a further evidence of the formation of a chemical bond between Si and Au.

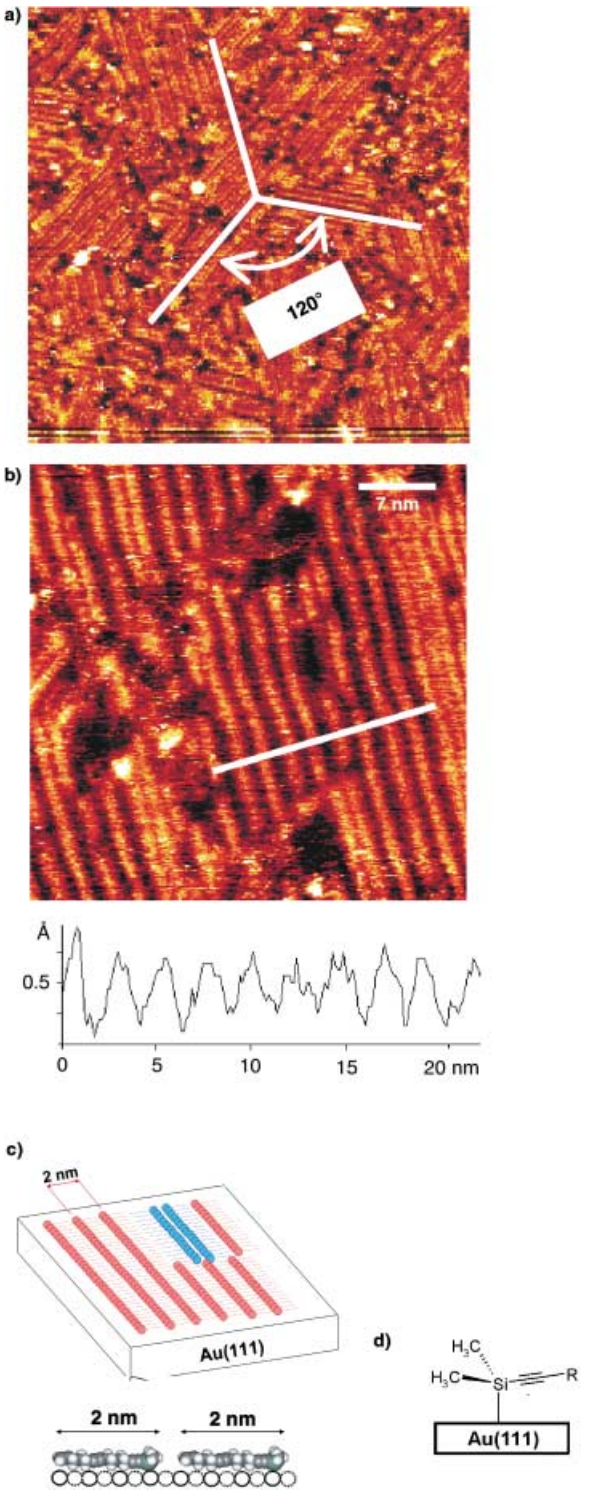

Figure 6. a) Self-assembly of molecule **7** at the Au(111)/*n*-tetradecane interface observed by STM (150×150 nm^2; $I_t = 0.618$ pA; $U_t = 189$V). The mosaic-like structure contains separated domains aligned along three preferential directions at 120° marked by white lines. b) STM image (40×40 nm^2; $I_t = 189$ pA; $U_t = 0.553$ V) of the close-packed arrangement of lamellae of compound **7** and their corresponding cross-sectional profile recorded along the white line. c) Two schematic side-views of the overlayer structure of **7** on Au(111) along one of the three observed directions. Both the predominant head-to-tail (red) and minority head-to-head (blue) arrangements observed in self-assembly of molecule **7** are represented here. d) Possible bonding configuration for molecule **7** on Au(111) involving elimination of the hydrogen atom.

The nature of the TMSA/gold interaction: In the light of the above results, it is now possible to refine our interpretation of the nature of the molecule–substrate interaction. The interaction between the TMSA compounds **1**–**4** and gold is certainly affected by the van der Waals stabilization induced by the perfect commensurability of the organic adlayer on the Au(111) lattice. However, our STM results (in particular the creation of pit holes and high stability) also confirm that a chemical reaction between Si and Au atoms has occurred. The hypothesis that we recently proposed of the formation of a local surface complex between TMSA and gold now appears very credible.[18] One possible mechanism is based on the activation of the Si atom by an electron-withdrawing and sterically compact group (like the C≡C triple bond of the TMSA motif). Such an activated Si atom can then become pentacoordinate and adopt a bipyramidal geometry when in contact with an electron-donating atom (such as Au).[39] Along this line, the most likely binding configuration of the surface complex formed between silane **1** and Au(111) is represented in Scheme 4. The three methyl groups would then be in a plane parallel to the surface plane, the linear polyunsaturated chain standing upright above the pentacoordinate Si atom. To our knowledge, this is the first report of such a local surface complex. In a further step, we now plan to investigate the nature of the Si–Au bond by means of surface spectroscopy techniques, for example, X-ray photoelectron spectroscopy.

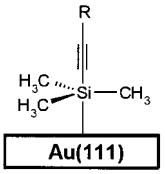

Scheme 4. Possible binding configuration for TMSA-based silane **1** on Au(111) involving a pentacoordinated Si atom in a bipyramidal geometry.

Conclusion

We have developed a molecular approach aimed at understanding the self-assembly mechanism of multifunctional linear TMSA compounds on reconstructed Au(111). We have synthesized a series of eight polyunsaturated organosilane homologues, each with slightly different chemical structures, and investigated their respective self-assembly properties by means of STM at the *n*-tetradecane/Au(111) interface. We show that all synthesized TMSA-terminated silanes self-assemble on gold in an upright position under the combined actions of 1) commensurability of the TMSA head with the gold adlattice and 2) creation of a surface Si–Au chemical bond.

The unique combination of these two features ensures that the resulting SAMs have an exceptional stability and long-range ordering. A slight chemical modification of the TMSA moiety generally leads to disordered layers, either by breaking commensurability (introduction of a bulky substituent on the TMSA head) or deactivating the chemical reactivity of Si with Au (removal of the adjacent C≡C triple bond). Substitution of one methyl group of TMSA by a hydrogen atom provides an activated SiR_3H compound with an asymmetrical silyl end-group. This interesting multifunctional linear silane self-assembles on gold with the molecules lying flat on the surface and aligned in lamellae oriented along either of the three preferential directions of the threefold symmetry Au(111) in a quasi-epitaxy mode.

Taking advantage of their remarkable stability, we are now investigating the electrical and optical properties of these new TMSA-based SAMs by various techniques. In particular, we will study the STM-induced photon emission at the liquid/solid interface as well as transport properties by scanning tunnelling spectroscopy. We have also started investigations on the nature of the chemical bond between Si and Au by means of X-ray photoelectron spectroscopy using a synchrotron source. Finally, TMSA-based SAMs are also promising for nanopatterning applications with the possibility to write motifs down to the molecular scale.

Experimental Section

Synthesis

General methods: Reactions were carried out under argon. Diethyl ether and THF were distilled from sodium/benzophenone under nitrogen before use. CH_2Cl_2 was dried and distilled from CaH_2. HMPA was distilled under reduced pressure after drying with CaH_2. Thin-layer chromatography (TLC) was performed on Merck $60F_{254}$ silica gel. Merck Geduran SI 60A silica gel (35–70 μm) was used for column chromatography; PE and EE refer to petroleum ether and diethyl ether, respectively. IR spectra were recorded with a Perkin–Elmer 1420 spectrometer. ^{1}H NMR and ^{13}C NMR spectra were recorded with 400 MHz ARX 400 Bruker spectrometer, chemical shifts are given in ppm, referenced to the residual proton resonances of the solvent ($\delta = 7.26$ ppm for $CDCl_3$). Coupling constants (J) are given in Hertz (Hz). The terms m, s, brs, d, t, q, and quint refer to multiplet, singlet, broad singlet , doublet, triplet, quadruplet, and quintuplet, respectively. All reactions were worked up as the following general procedure : dilution with Et_2O, washing with a saturated solution of NH_4Cl and brine, dried over Na_2SO_4, filtered, and concentrated in vacuo.

For further details of the synthesis see the Supporting Information.

Surface preparation: Gold substrates were prepared from gold films (thickness ≈150 nm) deposited in ultra high vacuum ($\sim 5 \times 10^{-8}$ Pa) onto a freshly cleaved mica surface heated at ~600 K. Reconstruction of the Au(111) surface was ensured by a careful annealing of the gold films in a gas flame (propane–air) and were systematically checked by STM before sample deposition. A small quantity of the organic compound (~ 0.05 mg mL^{-1}) was then mixed in *n*-tetradecane (99 + % purity, Aldrich), and a droplet of this solution was deposited onto the Au(111) substrate.

Scanning tunneling microscopy: STM images of bare gold and compounds **1**–**8** deposited on gold were recorded in *n*-tetradecane at room temperature (293–298 K) by using a Pico-SPM (Molecular Imaging). The STM tip was a Pt/Ir (80:20) wire sharpened by mechanical cutting. The experimental error in the measured lateral distances was within 5%. Multiple STM images recorded in the constant-current mode were obtained with different samples and conditions to test for reproducibility and ensure that the results were free of tip and sample artefacts. All STM images were flattened by software routines.

Acknowledgement

A.M. is grateful to CNRS-Département des Sciences Chimiques for financial support. Permanent address: Institute of Physics, Prospect Nauki 46, 252022, Kiev (Ukraine).

[1] A. Ulman, *Introduction to Ultratrathin Organic Films from Langmuir–Blodgett to Self-Assembly*, Academic Press, San Diego, CA, **1991**.
[2] L. Haussling, W. Knoll, H. Ringsdorf, F.-J. Schmitt, J. Yang, *Makromol. Chem. Macromol. Symp.* **1991**, *46*, 145.
[3] A. Kumar, G. M. Whitesides, *Science* **1994**, *263*, 60–62.
[4] J. K. Schoer, R. M. Crooks, *Langmuir* **1997**, *13*, 2323–2332.
[5] J. W. Zhao, K. Uosaki, *Nano Lett.* **2002**, *2*, 137–140.
[6] J. M. Tour, L. Jones, D. L. Pearson, J. J. S. Lamba, T. P. Burgin, G. M. Whitesides, D. L. Allara, A. N. Parikh, S. Atre, *J. Am. Chem. Soc.* **1995**, *117*, 9529–9534.
[7] T. Kondo, M. Yanagida, X. Q. Zhang, K. Uosaki, *Chem. Lett.* **2000**, 964–965.
[8] J. Collet, O. Tharaud, A. Chapoton, D. Vuillaume, *Appl. Phys. Lett.* **2000**, *76*, 1941–1943.
[9] A. Ulman, *Chem. Rev.* **1996**, *96*, 1533–1554
[10] G. E. Poirier, *Chem. Rev.* **1997**, *97*, 1117–1127.
[11] H. Takiguchi, K. Sato, T. Ishida, K. Abe, K. Yase, K. Tamada, *Langmuir* **2000**, *16*, 1703–1710.
[12] K. Tamada, T. Ishida, W. Knoll, H. Fukushima, R. Colorado, M. Graupe, O. E. Shmakova, T. R. Lee, *Langmuir* **2001**, *17*, 1913–1921.
[13] D. E. Hooks, T. Fritz, M. D. Ward, *Adv. Mater.* **2001**, *13*, 227–241.
[14] K. R. Finnie, R. Haasch, R. G. Nuzzo, *Langmuir* **2000**, *16*, 6968–6976.
[15] H. Sugimura, N. Nakagiri, *Nanotechnology* **1997**, *8*, A15–A18.
[16] a) O. Marchenko, J. Cousty, *Phys. Rev. Lett.* **2000**, *84*, 5363–5366; b) A. Marchenko, J. Cousty, L. Pham Van, *Langmuir* **2002**, *18*, 1171–1175.
[17] a) K. Uosaki, R. Yamada, *J. Am.Chem. Soc.* **1999**, *121*, 4090–4091; b) R. Yamada, K. Uosaki, *J. Phys. Chem. B* **2000**, *104*, 6021–6027.
[18] A. Marchenko, N. Katsonis, D. Fichou, C. Aubert and M. Malacria, *J. Am. Chem. Soc.* **2002**, *124*, 9998–9999.
[19] T. M. Owens, K. T. Nicholson, M. M. B. Holl, S. Suzer, *J. Am. Chem. Soc.* **2002**, *124*, 6800–6801.
[20] E. D. Sternberg, K. P. C. Vollhardt, *J. Org. Chem.* **1984**, *49*, 1574–1583.
[21] a) A. Dhirani, R. W. Zehner, R. P. Hsung, P. Guyot-Sionnest, L. R. Sita, *J. Am. Chem. Soc.* **1996**, *118*, 3319–3320; b) A. Dhirani, P.-H. Lin, P. Guyot-Sionnest, R. W. Zehner, L. R. Sita, *J. Chem. Phys.* **1997**, *106*, 5249–5253
[22] a) F. Slowinski, C. Aubert, M. Malacria, *Tetrahedron Lett.* **1999**, *40*, 707–710; b) C. Aubert; O. Buisine, M. Petit, F. Slowinski, M. Malacria, *Pure Appl. Chem.* **1999**, *71*, 1463–1470.
[23] F. Slowinski, C. Aubert, M. Malacria, *Eur. J. Org. Chem.* **2001**, 3491–3500.
[24] D. Craig, D. A. Fisher, O. Kermal, A. Marsh, T. Plessner, A. M. Z. Slawin, D. J. Williams, *Tetrahedron* **1991**, *47*, 3095–3128.
[25] A. J. Mancuso, S. L. Huang, D. Swern, *J. Org. Chem.* **1978**, *43*, 2480–2482.
[26] E. J. Corey. and P. L. Fuchs, *Tetrahedron Lett.* **1972**, 3769–3772.
[27] J. S. Foster, J. E. Frommer, *Nature* **1988**, *333*, 542–545.
[28] D. M. Cyr, B. Venkataraman, G. W. Flynn, *Chem. Mater.* **1996**, *8*, 1600–1615.
[29] R. Yamada, K. Uosaki, *Langmuir* **1998**, *14*, 855–861.
[30] G. M. Watson, D. Gibbs, S. Song, A. R. Sandy, S. G. J. Mochrie, D. M. Zehner, *Phys. Rev. B* **1995**, *52*, 12329–12344.
[31] A. Marchenko, Z. X. Xie, J. Cousty, L. Pham Van, *Surf. Interface Anal.* **2000**, *30*, 167–169.
[32] a) O. Chailapakul, L. Sun, C. Xu, R. M. Crooks, *J. Am. Chem. Soc.* **1993**, *115*, 12459–12467; b) E. Delamarche, B. Michel, H. Kang, C. Gerber, *Langmuir* **1994**, *10*, 4103–4108; c) O. Cavalleri, H. Hirstein, K. Kern, *Surf. Sci.* **1995**, *340*, L960–L964.
[33] a) K. Edinger, A. Goelzhaeuser, K. Demota, C. Woell, M. Grunze, *Langmuir* **1993**, *9*, 4–8; b) J-P. Bucher, L. Santesson, K. Kern, *Langmuir* **1994**, *10*, 979–983.
[34] U. Durig, O. Zuger, B. Michel, L. Haussling, H. Ringsdorf, *Phys. Rev. B* **1993**, *48*, 1711–1717.
[35] M. D. Mowery, H. Menzel, M. Cai, C. E. Evans, *Langmuir* **1998**, *14*, 5594–5602.
[36] J. E. Anthony, D. L. Eaton, S. R. Parkin, *Org. Lett.* **2002**, *4*, 15–18.
[37] N. B. Larsen, H. Biebuyck, E. Delamarche, B. Michel, *J. Am. Chem. Soc.* **1997**, *119*, 3017–3026.
[38] Q. M. Xu, L. J. Wan, S. X. Yin, C. Wang, C. L. Bai, T. Ishii, K. Uehara, Z. Y. Wang, T. Nozawa, *J. Phys. Chem. B* **2002**, *106*, 3037–3040.
[39] a) C. Chuit, R. J. P. Corriu, C. Reye, J. C. Young, *Chem. Rev.* **1993**, *93*, 1371–1448; b) S. E. Denmark, B. D. Griedel, D. M. Coe, M. E. Schnute, *J. Am. Chem. Soc.* **1994**, *116*, 7026–7043.

Received: December 18, 2002 [F4682]

